Relativistic models for quasi-elastic neutrino-nucleus scattering

Andrea Meucci

Dipartimento di Fisica Nucleare e Teorica - Università di Pavia
INFN - Sezione di Pavia

Trento - Dicembre 2011

Introduction

- ♡ : Charged- and Neutral-Current neutrino-nucleus scattering
- ♠ : relativistic models for neutrino-nucleus scattering
- ♢ : some results for CC neutrino-nucleus scattering and scaling
- ♣ : results for the MiniBooNE CCQE cross sections
- ♡ : results for the MiniBooNE NCE cross sections
- ♠ : Collaborators C. Giusti, F.D. Pacati, M.B. Barbaro, J.A. Caballero, J.M. Udías

ν-nucleus scattering

$$\left.\begin{aligned} \nu_\mu(\bar\nu_\mu) + A &\longrightarrow \mu^-(\mu^+) + N + (A-1) \\ \nu_\mu(\bar\nu_\mu) + A &\longrightarrow \nu_\mu(\bar\nu_\mu) + N + (A-1) \end{aligned}\right\} \quad \text{CC and NC scattering!}$$

$$\mathrm{d}\sigma = \frac{G_\mathrm{F}^2}{2}\, 2\pi\, L^{\mu\nu}\, W_{\mu\nu}\, \frac{\mathrm{d}^3 k}{(2\pi)^3}\, \frac{\mathrm{d}^3 p_\mathrm{N}}{(2\pi)^3}$$

♡ : lepton tensor

$$L^{\mu\nu} = \frac{2}{\varepsilon_i \varepsilon}\left[l_S^{\mu\nu} \mp l_A^{\mu\nu}\right] \quad \begin{pmatrix} \nu \text{ scattering} \\ \bar\nu \text{ scattering} \end{pmatrix}$$

♠ : $G_\mathrm{F} \simeq 1.16639 \times 10^{-11}$ MeV^{-2} Fermi constant ($\times \cos^2\vartheta_\mathrm{C} \simeq 0.9749$ for CC scattering)

♢ : hadron tensor

$$W^{\mu\nu}(q,\omega) = \overline{\sum_i} \,\, \sum\!\!\!\!\!\!\!\int_f \langle \Psi_f \mid \hat{J}^\mu(\boldsymbol{q}) \mid \Psi_0\rangle \langle \Psi_0 \mid \hat{J}^{\nu\dagger}(\boldsymbol{q}) \mid \Psi_f\rangle \, \delta(E_0 + \omega - E_f),$$

weak current

♡ : charged current

$$j^\mu = \left[F_1^{\rm V}(Q^2)\gamma^\mu + i\frac{\kappa}{2M}F_2^{\rm V}(Q^2)\sigma^{\mu\nu}q_\nu - G_{\rm A}(Q^2)\gamma^\mu\gamma^5 + F_{\rm P}(Q^2)q^\mu\gamma^5\right]\tau^\pm$$

♠ : vector form factor

$$F_i^{\rm V} = F_i^{\rm p} - F_i^{\rm n}$$

♢ : axial form factor

$$G_{\rm A} = g_{\rm A}G = \frac{1.26}{(1+Q^2/M_{\rm A}^2)^2}$$

♣ : pseudo-scalar form factor

$$F_{\rm P} = \frac{2Mg_{\rm A}G}{m_\pi^2 + Q^2}$$

♡ : neutral current

$$j^\mu = F_1^{\rm V}(Q^2)\gamma^\mu + i\frac{\kappa}{2M}F_2^{\rm V}(Q^2)\sigma^{\mu\nu}q_\nu - G_{\rm A}(Q^2)\gamma^\mu\gamma^5$$

♣ : strange form factors

$$F_i^{\rm V,p(n)} = \left(1/2 - 2\sin^2\theta_{\rm W}\right)F_i^{\rm p(n)} - 1/2F_i^{\rm n(p)} - 1/2F_i^{\rm s}$$

$$G_{\rm A} = \frac{1}{2}(\tau_3 g_{\rm A} - \Delta s)\,G$$

$$F_1^{\rm s}(Q^2) = \frac{(\rho^{\rm s} + \mu^{\rm s})\tau}{(1+\tau)(1+Q^2/M_{\rm V}^2)^2} \qquad F_2^{\rm s}(Q^2) = \frac{(\mu^{\rm s} - \tau\rho^{\rm s})}{(1+\tau)(1+Q^2/M_{\rm V}^2)^2}$$

NC ν-nucleus cross section

$$\frac{\mathrm{d}\sigma}{\mathrm{d}\epsilon\,\mathrm{d}\Omega\,\mathrm{d}T_{\mathrm{N}}} = \frac{G_F^2}{2\pi^2}\,\epsilon^2\cos^2\frac{\theta}{2}\Big[v_0 R_{00} + v_{zz}R_{zz} - v_{0z}R_{0z} + v_T R_T \pm v_{xy}R_{xy}\Big]\frac{|\boldsymbol{p}_{\mathrm{N}}|E_{\mathrm{N}}}{(2\pi)^3}\ ,$$

♡ : lepton tensor components ⟵ (the mass of the outgoing lepton is neglected)

$$v_0 = 1\ ,\quad v_{zz} = \frac{\omega^2}{|\boldsymbol{q}|^2}\ ,\quad v_{0z} = \frac{\omega}{|\boldsymbol{q}|},$$

$$v_T = \tan^2\frac{\theta}{2} + \frac{Q^2}{2|\boldsymbol{q}|^2}\ ,\qquad v_{xy} = \tan\frac{\theta}{2}\sqrt{\left[\tan^2\frac{\theta}{2} + \frac{Q^2}{|\boldsymbol{q}|^2}\right]}\ ,$$

♠ : response functions

$$R_{00} = \int \mathrm{d}\Omega_{\mathrm{N}}\,W^{00}\ ,\quad R_{zz} = \int \mathrm{d}\Omega_{\mathrm{N}}\,W^{zz}\ ,\quad R_{0z} = \int \mathrm{d}\Omega_{\mathrm{N}}\,2\,\mathrm{Re}(W^{0z})\ ,$$

$$R_T = \int \mathrm{d}\Omega_{\mathrm{N}}\,(W^{xx} + W^{yy})\ ,\quad R_{xy} = \int \mathrm{d}\Omega_{\mathrm{N}}\,2\,\mathrm{Im}\,(W^{xy})\ .$$

the transition amplitude in RDWIA

♡ : The components of the hadron tensor can be expressed as

$$W^{\mu\nu}(q,\omega) \quad = \quad \overline{\sum_i} \sum\!\!\!\!\!\!\int_f \langle \Psi_f \mid \hat{J}^{\mu}(\boldsymbol{q}) \mid \Psi_0\rangle\langle\Psi_0 \mid \hat{J}^{\nu\dagger}(\boldsymbol{q}) \mid \Psi_f\rangle\ \delta(E_0+\omega-E_f),$$

♠ : The matrix elements of the nuclear current operator are expressed in the IA as the sum, over all the single-particle states, of the squared absolute value of the transition matrix elements of the single-nucleon current

$$\langle\chi^{(-)}(E) \mid j^{\mu} \mid \varphi_n(E)\rangle \ ,$$

and are calculated with relativistic wave functions $\Longrightarrow$ same treatment as in $(e, e'p)$ calculations.

♢ : $\varphi_n \Longrightarrow$ Dirac-Hartree solutions of a relativistic mean field theory Lagrangian

♣ : Scattering wave function $\chi^{(-)}(E) \Longrightarrow$ we write it in terms of its positive energy components

$$\chi^{(-)}(E) = \begin{pmatrix} \Psi_{\mathrm{f}+} \\ \dfrac{1}{M+E+S^{\dagger}(E)-V^{\dagger}(E)}\boldsymbol{\sigma}\cdot\boldsymbol{p}\Psi_{\mathrm{f}+} \end{pmatrix} ,$$

♡ : Ψ_{f+} is related to a Schrödinger-like wave function, Φ_f, by the Darwin factor, i.e.,

$$\Psi_{f+} = \sqrt{D^{\dagger}(E)}\Phi_f \ , \quad D(E) = 1 + \frac{S(E)-V(E)}{M+E}$$

.

♠ : RDWIA $\Longrightarrow$ FSI effects are accounted for by solving the Dirac equation with strong relativistic scalar and vector optical potentials.

CC ν-nucleus cross section

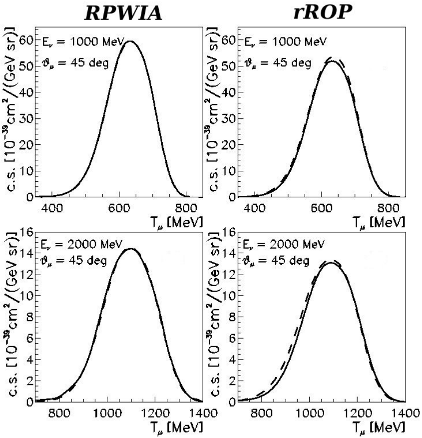

♡ : comparison of the results of the different relativistic models developed by the Pavia and the Madrid-Sevilla groups in the same conditions

♠ : ^{12}C(ν_μ, μ^-) @ $E_\nu = 1000, 2000$ MeV and $\vartheta_\mu = 45^o$

♢ : RPWIA $\Longrightarrow$ FSI are neglected

♣ : rROP $\Longrightarrow$ the imaginary part of the phenomenological relativistic energy dependent optical potentials is set to zero

♡ : see A. Meucci, J.A. Caballero, C. Giusti, J.M. Udías, Phys. Rev. C **83**, 064614 (2011).

CC ν-nucleus cross section (2)

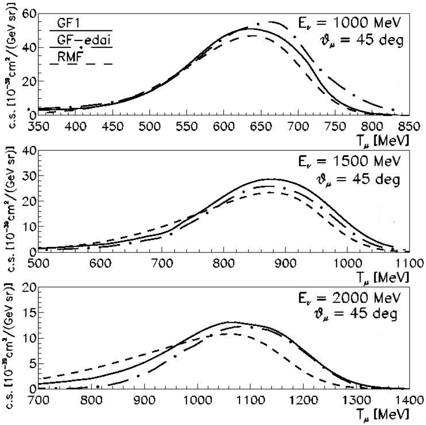

♡ : comparison of the results obtained in the RGF and RMF by the Pavia and Madrid-Sevilla groups

♠ : ^{12}C(ν_μ, μ^-) @ $E_\nu = 1000, 1500, 2000$ MeV and $\vartheta_\mu = 45^o$

♢ : RGF → relativistic Green's function $\Longrightarrow$ consistent treatment of FSI in the exclusive and in the inclusive scattering

♣ : RMF $\Longrightarrow$ the scattering states are described by using the same real scalar and vector relativistic mean field potentials considered in the description of the initial bound state

♡ : see A. Meucci, J.A. Caballero, C. Giusti, J.M. Udías, Phys. Rev. C **83**, 064614 (2011).

CC ν-nucleus cross section (3)

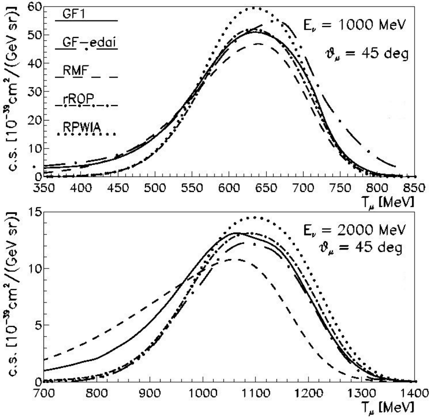

♡ : general comparison of our results

♠ : ^{12}C(ν_μ, μ^-) @ $E_\nu = 1000, 2000$ MeV and $\vartheta_\mu = 45^o$

♢ : RGF $\Longrightarrow$ differences between GF1 and GF-EDAI depend on the energy and momentum transfer $\rightarrow$ structure of the energy-dependent relativistic optical potentials adopted in the RGF model

♣ : RMF $\Longrightarrow$ differences with RGF results increase with the energy and momentum transfer $\rightarrow$ ingredients of these calculations

♡ : RMF and RGF $\Longrightarrow$ asymmetry with a tail extended to large ω = small T_μ

♠ : RGF may account for in a phenomenological way additional effects due to non-nucleonic degrees of freedom

♢ : RPWIA and rROP $\longrightarrow$ symmetric shape

♣ : see A. Meucci, J.A. Caballero, C. Giusti, J.M. Udías, Phys. Rev. C **83**, 064614 (2011).

CC ν-nucleus cross section (4)

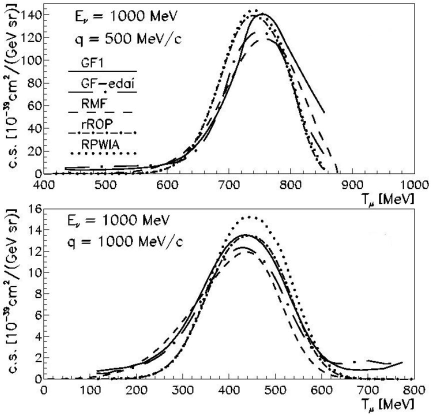

♡ : general comparison of our results in a kinematics more similar to (e, e')

♠ : ^{12}C(ν_μ, μ^-) @ $E_\nu = 1000$ MeV and $q = 500$ and 1000 MeV

♢ : RGF and RMF $\Longrightarrow$ asymmetric shape toward high ω = small T_μ

♣ : differences between GF1 and GF-EDAI $\rightarrow$ structure of the energy-dependent relativistic optical potentials adopted in the RGF model

♡ : differences between RMF and RGF increase with E_ν and q $\rightarrow$ ingredients of these calculations

♠ : RPWIA and rROP

♢ : see A. Meucci, J.A. Caballero, C. Giusti, J.M. Udías, Phys. Rev. C **83**, 064614 (2011).

CC ν-nucleus and scaling

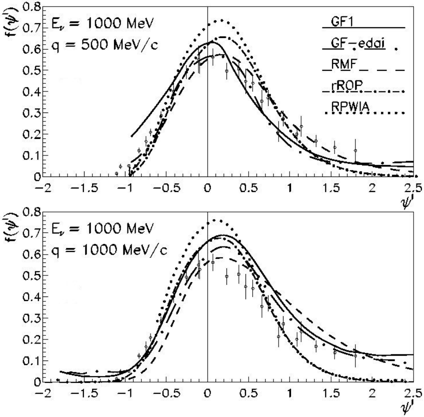

♡ : general comparison of our results for the scaling functions extracted from the cross sections see J. A. Caballero, *et al.* ,Phys. Rev. Lett. **95**, 252502 (2005)

♠ : ^{12}C(ν_μ, μ^-) @ $E_\nu = 1000$ MeV and $q = 500$ and 1000 MeV

♢ : RMF $\Longrightarrow$ explains the asymmetric behavior of the phenomenolgical scaling function and is in accordance with the longitudinal scaling function extracted from the (e, e') reaction

♣ : RGF $\Longrightarrow$ reasonable agreement with the averaged experimental scaling function

♡ : RPWIA and rROP

♠ : see A. Meucci, J.A. Caballero, C. Giusti, J.M. Udías, Phys. Rev. C **83**, 064614 (2011).

CC ν-nucleus and scaling (2)

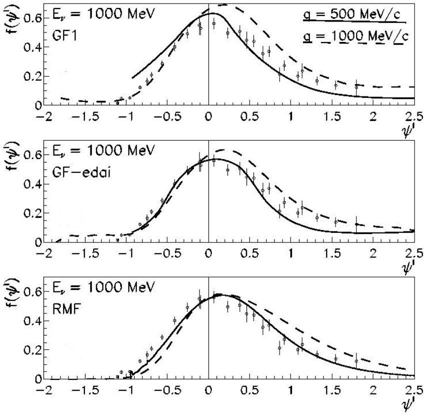

♡ : analysis of first kind scaling (independence of the momentum transfer) with our results in a kinematics more similar to (e, e')

♠ : ^{12}C(ν_μ, μ^-) @ $E_\nu = 1000$ MeV and $q = 500$ and 1000 MeV

♢ : RMF $\Longrightarrow$ slight shift in the region $\psi' < 0$ whereas the model breaks scaling approximately at 30% when $\psi' > 0$

♣ : RGF $\Longrightarrow$ similar to RMF but the stronger scaling breakdown shown by RGF may reflect the effective presence of non-nucleonic contributions

♡ : see A. Meucci, J.A. Caballero, C. Giusti, J.M. Udías, Phys. Rev. C **83**, 064614 (2011).

The MiniBooNE CCQE results

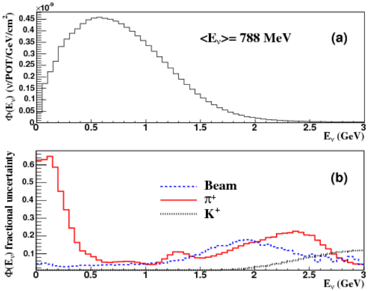

♡ : Muon neutrino flux at the MiniBooNE detector as a function of neutrino energy along with the fractional uncertainties grouped into various contributions

♢ : see A.A. Aguilar-Arevalo, *et al.*, Phys. Rev. D **81**, 092005 (2010).

♠ : The MiniBooNE Collaboration performed a high statistics measurement of the flux-averaged double differential cross section

$$\frac{d^2\sigma}{dT_\mu d\cos\theta_\mu}$$

♣ : flux-integrated CCQE single differential cross section

$$\frac{d\sigma}{dQ_{QE}}$$

♠ : flux-unfolded CCQE cross section as a function of energy

$$\sigma\left[E_\nu^{QE,RFG}\right]$$

The MiniBooNE CCQE cross section

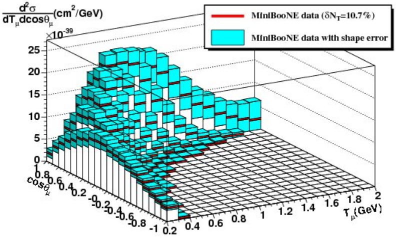

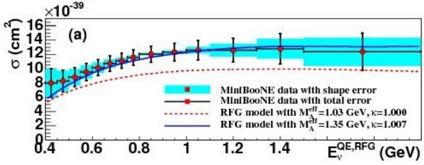

♡ : The MiniBooNE flux-integrated double differential cross section per target neutron for the ν_μ CCQE process

♠ : $M_A = 1.35 \pm 0.17$ GeV $\longrightarrow$ axial vector mass using just MiniBooNE data

♣ : Flux-unfolded MiniBooNE ν_μ CCQE cross section per neutron as a function of neutrino energy compared with predictions from the NUANCE simulation for an RFG model.

♢ : see A.A. Aguilar-Arevalo, *et al.*, Phys. Rev. D **81**, 092005 (2010).

Some questions raised by the MiniBooNE data

axial mass

♠ : $M_A = 1.39 \pm 0.11$ GeV $\longrightarrow$ axial vector mass using MiniBooNE NCE data

♢ : $M_A = 1.35 \pm 0.17$ GeV $\longrightarrow$ axial vector mass using MiniBooNE CCQE data

♣ : other neutrino measurements $M_A \approx 1.2 - 1.3$ GeV

♡ : $M_A = 1.03 \pm 0.02$ GeV world average value

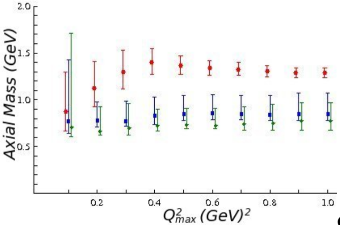

♠ : models including only one-nucleon knockout generally use $M_A \approx 1.3 - 1.4$ GeV

♢ : other models do not need to change $M_A = 1.03$ GeV $\rightarrow$: relativistic Green's function (and others)

♣ : see also J. Nieves, *et al.*, arXiv:1106.5374 [hep-ph] and M. Martini, *et al.*, Phys. Rev. C **84** 055502 (2011).

♠ : model-independent description of the axial-vector form factor

♢ : $M_A = 0.85^{+0.22}_{-0.07} \pm 0.09$ GeV

♣ : see B. Bhattacharya, *et al.*, Phys. Rev. D **84**, 073006 (2011).

Δs (NCE scattering)

♠ : $\Delta s = 0.08 \pm 0.26$

♢ : very interesting results but obtained assuming $M_A = 1.35$ GeV and neglecting G_E^s and G_M^s

MiniBooNE CCQE double differential cross section

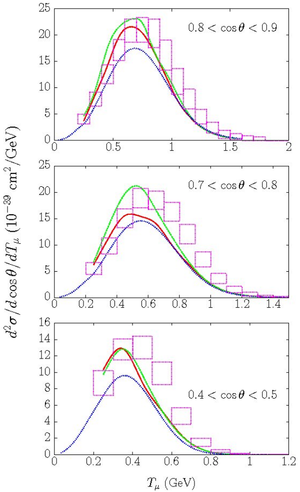

♡ : CCQE double differential cross section averaged over the neutrino flux as a function of the muon kinetic energy

♣ : 3 bins of cos θ

♢ : $M_A = 1.03$ GeV

♠ : RMF $\longrightarrow$ reasonable agreement with data for small θ and low T_μ

♡ : RGF $\longrightarrow$ results larger than the RMF and in reasonable agreement with data

♣ : see A. Meucci, M.B. Barbaro, J.A. Caballero, C.Giusti, J.M. Udías, Phys. Rev. Lett. **107**, 172501 (2011).

MiniBooNE CCQE double differential cross section

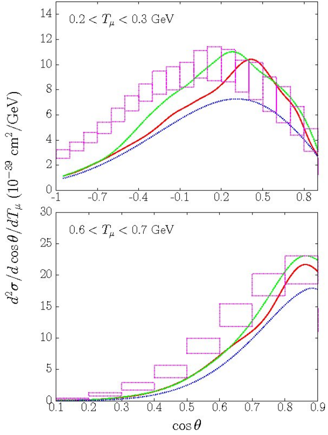

♡ : CCQE double differential cross section averaged over the neutrino flux as a function of cos θ

♣ : 2 bins of T_μ

♢ : $M_A = 1.03$ GeV

♠ : RMF $\longrightarrow$ underestimates the data for low T_μ and better agreement as T_μ increases

♡ : RGF $\longrightarrow$ results larger than the RMF and in reasonable agreement with data for small θ

♣ : see A. Meucci, M.B. Barbaro, J.A. Caballero, C.Giusti, J.M. Udías, Phys. Rev. Lett. **107**, 172501 (2011).

Flux-unfolded MiniBooNE ν_μ CCQE cross section

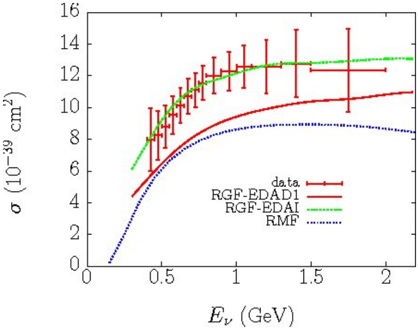

♡ : total CCQE cross section per neutron as a function of the neutrino energy

♣ : RMF and RGF

♢ : $M_A = 1.03$ GeV

♠ : differences between RGF-EDAI and RGF-EDAD1 $\longrightarrow$ different values of the imaginary parts of both potentials, particularly for the energies considered in kinematics with the lowest θ and the largest T_μ

♡ : see A. Meucci, M.B. Barbaro, J.A. Caballero, C.Giusti, J.M. Udías, Phys. Rev. Lett. **107**, 172501 (2011).

The MiniBooNE NCE results

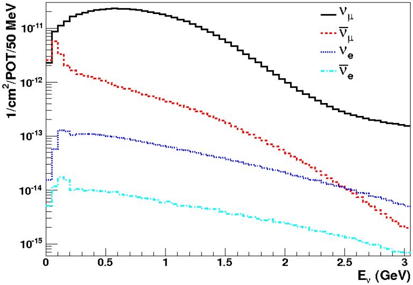

♡ : Neutrino flux at the MiniBooNE detector for different types of neutrinos as a function of their energy

♢ : see A.A. Aguilar-Arevalo, *et* al., Phys. Rev. D **82**, 092005 (2010).

♠ : The MiniBooNE Collaboration performed a high statistics measurement of the flux-averaged differential cross section as a function of Q^2 for NCE scattering on CH_2 for Q^2 up to 1.65 GeV^2.

♣ : The NCE cross section is presented as scattering from individual nucleons but consists of 3 different processes → scattering on free protons in H, bound protons and neutrons in C:

$$
\begin{aligned}
\frac{d\sigma_{\nu N\to\nu N}}{dQ^2} &= \frac{1}{7}\, C_{\nu p,H}(Q^2_{QE})\, \frac{d\sigma_{\nu p\to\nu p,H}}{dQ^2} \\
&+ \frac{3}{7}\, C_{\nu p,C}(Q^2_{QE})\, \frac{d\sigma_{\nu p\to\nu p,C}}{dQ^2} \\
&+ \frac{3}{7}\, C_{\nu n,C}(Q^2_{QE})\, \frac{d\sigma_{\nu n\to\nu n,C}}{dQ^2},
\end{aligned}
$$

♠ : $d\sigma_{\nu p\to\nu p,C}/dQ^2$ NCE cross-section on bound protons per bound protons

♣ : $C_{\nu p,C}$ effieciency corrections

The MiniBooNE NCE cross section

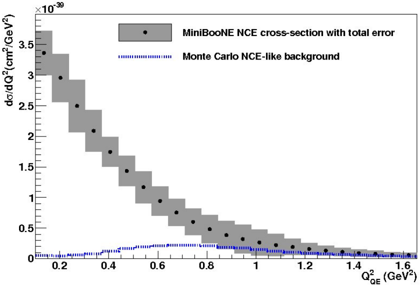

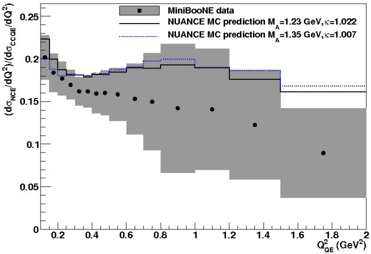

♡ : The MiniBooNE NCE ($\nu N \to \nu N$) flux-averaged differential cross section on CH_2

♠ : $M_A = 1.39 \pm 0.11$ GeV $\longrightarrow$ axial vector mass using MiniBooNE data

♣ : The MiniBooNE NCE/CCQE cross section ratio on CH_2

♢ : see A.A. Aguilar-Arevalo, *et* al., Phys. Rev. D **82**, 092005 (2010).

The MiniBooNE measurement of Δs

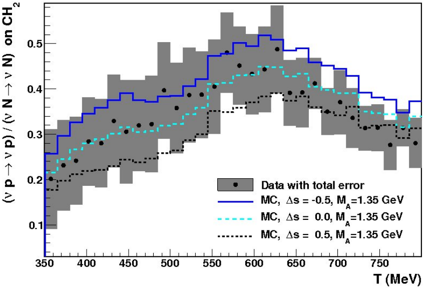

♠ : The ratio of $\nu p \to \nu p$ to $\nu N \to \nu N$ events for data compared with 3 MonteCarlo calculations for different values of Δs

♢ : see A.A. Aguilar-Arevalo, *e*t al., Phys. Rev. D **82**, 092005 (2010).

♠ : The MiniBooNE cross section do not depend on Δs

♡ : ratios of cross sections useful to extract Δs at low Q^2 with reduced systematic errors

♣ : in order to measure Δs, the ratio of $\nu p \to \nu p$ to $\nu N \to \nu N$ as a function of the reconstructed nucleon kinetic energy from 350 MeV to 800 MeV is used

♢ : $\Delta s = 0.08 \pm 0.26$

♠ : errors are quite large but it is the first attempt at a Δs determination using this ratio

MiniBooNE NCE cross section: RDWIA and RPWIA

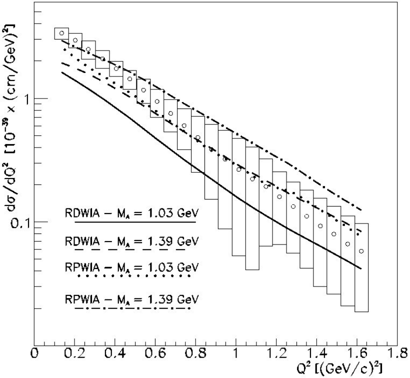

- ♡ : NCE flux-averaged ($\nu N \longrightarrow \nu N$) cross section
- ♠ : RDWIA and RPWIA
- ♢ : $M_A = 1.03$ GeV and $M_A = 1.39$ GeV
- ♣ : see A. Meucci, C.Giusti, F.D. Pacati, Phys. Rev. D **84**, 113003 (2011).

MiniBooNE NCE cross section: Δs

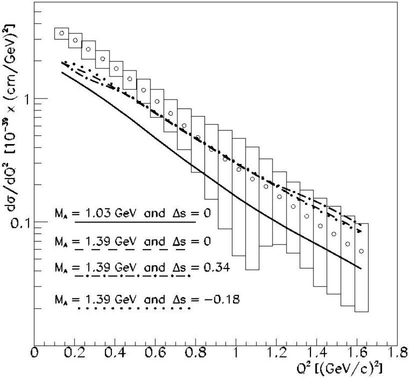

♡ : NCE flux-averaged ($\nu N \longrightarrow \nu N$) cross section

♣ : RDWIA

♢ : $M_A = 1.03$ GeV and $M_A = 1.39$ GeV

♠ : $\Delta s = -0.18$, $\Delta s = 0$, $\Delta s = 0.34$

♡ : negligible effect of $\Delta s \Longrightarrow$ compensation of effects

♣ : see A. Meucci, C.Giusti, F.D. Pacati, Phys. Rev. D **84**, 113003 (2011).

MiniBooNE NCE cross section: relativistic Green's function

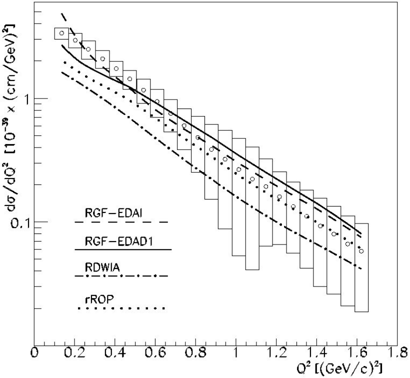

- ♡ : NCE flux-averaged ($\nu N \longrightarrow \nu N$) cross section
- ♣ : relativistic Green's function with 2 optical potentials
- ♢ : RDWIA and rROP
- ♠ : $M_A = 1.03$ GeV and $\Delta s = 0$
- ♡ : see A. Meucci, C.Giusti, F.D. Pacati, Phys. Rev. D **84**, 113003 (2011).

some comments ...

♡ : Green's function approach $\Longrightarrow$ the imaginary part of the optical potental redistributes the strength in all the channels and the total flux is conserved

♠ : The relativistic Green's function is suitable for an inclusive process like (e, e') or (ν_μ, μ^-)

♢ : NCE scattering $\Longrightarrow$ RGF can include also contributions of channels that are not included in a cross sections like the NCE MiniBooNE

♣ : RDWIA gives smaller results than the experimental data $\rightarrow$ the absorbitive imaginary part of the optical potential reduces the cross section $\Longrightarrow$ the contributions of some channels are neglected

♡ : The RPWIA, rROP, and RDWIA results underpredict the MiniBooNE NCE data (unless $M_A \approx 1.3 - 1.4$ GeV), while the RGF results are in reasonable agreement with them

♠ : possible contribution of reaction channels like re-scattering processes of the nucleon in its way out of the nucleus or non-nucleonic Δ excitations, which may arise during nucleon propagation, with or without real pion production, or also multinucleon processes $\Longrightarrow$ they are not included explicitly in the Green's function but can be recovered, to some extent, by the imaginary part of the phenomenological optical potential

♢ : Additional complication (1) $\Longrightarrow$ the flux-average procedure to evaluate the CCQE and NCE cross sections (convolution of the double differential cross section over the neutrino spectrum)

♣ : Additional complication (2) $\Longrightarrow$ the MiniBooNE NCE cross section is given in bins of Q^2 which is reconstructed from the kinetic energies of the ejected nucleons

♡ : see A. Meucci, C.Giusti, F.D. Pacati, Phys. Rev. D **84**, 113003 (2011).

MiniBooNE cross section: NCE/CCQE

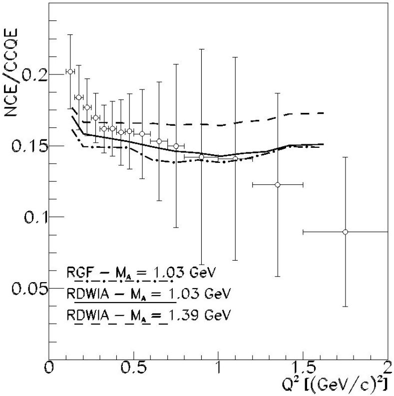

♡ : NCE/CCQE ratio as a function of Q^2

♣ : both NCE and CCQE cross sections are per target nucleon

♢ : ratios do not depend on final state interaction effets

♠ : the NCE/CCQE ratio was proposed as an attractive quantity to measure Δs

♡ : unuseful to measure $\Delta s \rightarrow$ NCE cross section do not depend on Δs

♣ : see A. Meucci, C.Giusti, F.D. Pacati, Phys. Rev. D **84**, 113003 (2011).

MiniBooNE cross section: proton knockout and Δs

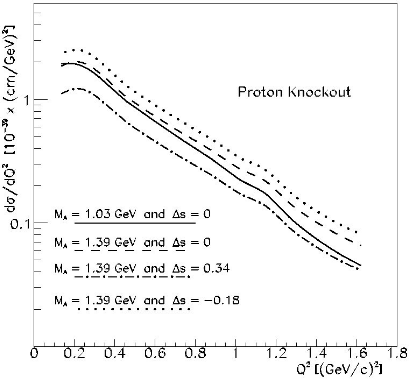

- ♡ : NCE flux-averaged ($\nu p \longrightarrow \nu p$) cross section
- ♣ : RDWIA
- ♢ : $M_A = 1.03$ GeV and $M_A = 1.39$ GeV
- ♠ : $\Delta s = -0.18$, $\Delta s = 0$, $\Delta s = 0.34$
- ♡ : visible effects of Δs but no comparison with experimental data
- ♣ : see A. Meucci, C.Giusti, F.D. Pacati, Phys. Rev. D **84**, 113003 (2011).

MiniBooNE cross section: neutron knockout and Δs

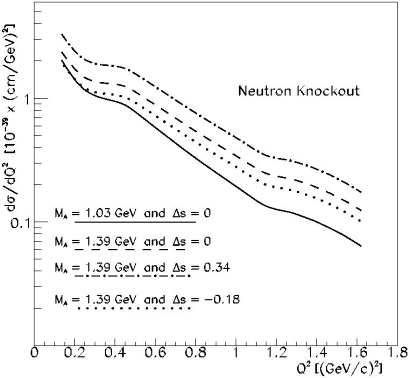

- ♡ : NCE flux-averaged ($\nu n \longrightarrow \nu n$) cross section
- ♣ : RDWIA
- ♢ : $M_A = 1.03$ GeV and $M_A = 1.39$ GeV
- ♠ : $\Delta s = -0.18$, $\Delta s = 0$, $\Delta s = 0.34$
- ♡ : visible effects of Δs but no comparison with experimental data
- ♣ : see A. Meucci, C.Giusti, F.D. Pacati, Phys. Rev. D **84**, 113003 (2011).

MiniBooNE cross section: ratio p/n and Δs

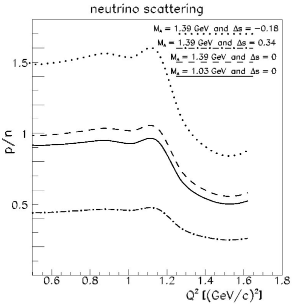

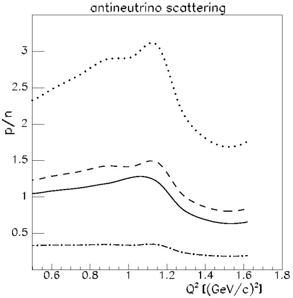

- ♡ : ratio of proton-to-neutron flux-averaged cross sections
- ♣ : RDWIA
- ♢ : $M_A = 1.03$ GeV and $M_A = 1.39$ GeV
- ♠ : $\Delta s = -0.18$, $\Delta s = 0$, $\Delta s = 0.34$
- ♡ : visible effects of Δs but no comparison with experimental data
- ♣ : neutrino and antineutrino scattering $\Longrightarrow$ similar results
- ♢ : see A. Meucci, C.Giusti, F.D. Pacati, Phys. Rev. D **84**, 113003 (2011).

the relativistic Green's function approach

♡ : For an inclusive process the components of the hadron tensor can be expressed as

$$W^{\mu\nu} = \langle \Psi_0 \mid J^{\nu\,\dagger} \delta\left(E_{\mathrm{f}} - H\right) J^{\mu} \mid \Psi_0 \rangle$$

♠ : The components of $W^{\mu\nu}$ can be re-expressed in terms of the Green's operators related to the nuclear Hamiltonian H. For example (for $\mu = 0, x, y, z$)

$$\omega^{\mu\mu} = W^{\mu\mu} = -\frac{1}{\pi}\mathrm{Im}\langle \Psi_0 \mid J^{\mu\,\dagger} G(E_{\mathrm{f}}) J^{\mu} \mid \Psi_0 \rangle$$

♢ : The components of the nuclear response can be written in terms of the single-particle Green's function $\mathcal{G}(E)$, whose self-energy is the Feshbach's optical potential.

♣ : An explicit calculation of the Green's function can be avoided by its spectral representation, which is based on a biorthogonal expansion in terms of the eigenfunctions of the non-Hermitian optical potential $\mathcal{V}$, and of its Hermitian conjugate $\mathcal{V}^{\dagger}$, i.e.,

$$\left[\mathcal{E} - T - \mathcal{V}^{\dagger}(E)\right] \mid \chi_{\mathcal{E}}^{(-)}(E)\rangle = 0\,, \quad \left[\mathcal{E} - T - \mathcal{V}(E)\right] \mid \tilde{\chi}_{\mathcal{E}}^{(-)}(E)\rangle = 0\,.$$

spectral representation of the hadron tensor

♡ : spectral representation of the Green's function:

$$\mathcal{G}(E) = \int_M^\infty \mathrm{d}\mathcal{E} \mid \tilde{\chi}_{\mathcal{E}}^{(-)}(E)\rangle \frac{1}{E - \mathcal{E} + i\eta} \langle \chi_{\mathcal{E}}^{(-)}(E) \mid$$

♠ : expanded form for the single particle expressions of the hadron tensor components

$$\omega^{\mu\nu}(\omega, q) = -\frac{1}{\pi} \sum_n \mathrm{Im}\left[\int_M^\infty \mathrm{d}\mathcal{E} \frac{1}{E_\mathrm{f} - \epsilon_n - \mathcal{E} + i\eta} T_n^{\mu\nu}(\mathcal{E}, E_\mathrm{f} - \epsilon_n) \right]$$

$$T_n^{\mu\mu}(\mathcal{E}, E) = \lambda_n \langle \varphi_n \mid j^{\mu\dagger}(\boldsymbol{q}) \sqrt{1 - \mathcal{V}'(E)} \mid \tilde{\chi}_{\mathcal{E}}^{(-)}(E)\rangle\langle \chi_{\mathcal{E}}^{(-)}(E) \mid \sqrt{1 - \mathcal{V}'(E)} j^\mu(\boldsymbol{q}) \mid \varphi_n\rangle$$

♢ : similar expressions for the terms with $\mu \neq \nu$

♣ : expanded form for the hadron tensor components

$$\omega^{\mu\nu}(\omega, q) = \sum_n \left[\mathrm{Re}\, T_n^{\mu\nu}(E_\mathrm{f} - \epsilon_n, E_\mathrm{f} - \epsilon_n) - \frac{1}{\pi} \mathcal{P} \int_M^\infty \mathrm{d}\mathcal{E} \frac{1}{E_\mathrm{f} - \epsilon_n - \mathcal{E}} \mathrm{Im}\, T_n^{\mu\nu}(\mathcal{E}, E_\mathrm{f} - \epsilon_n) \right]$$

- $\lim_{\eta \to 0} \frac{1}{E - \mathcal{E} + i\eta} = \mathcal{P}\left(\frac{1}{E - \mathcal{E}}\right) - i\pi\delta\left(E - \mathcal{E}\right)$
- $\sqrt{1 - \mathcal{V}'(E)}$ accounts for interference effects between different channels and allows the replacement of the mean field $\mathcal{V}$ with the phenomenological optical potential $\mathcal{V}_\mathrm{L}$

comments ...

♡ : $\sqrt{\lambda_n}\langle\chi_{\mathcal{E}}^{(-)}(E) \mid j^{\mu}(\boldsymbol{q}) \mid \varphi_n\rangle \Longrightarrow$ transition amplitude for the single-nucleon knockout from a nucleus in the state $\mid \Psi_0\rangle$ leaving the residual nucleus in the state $\mid n\rangle$
$\Longrightarrow$ attenuation of the strength due to imaginary part of $\mathcal{V}^{\dagger}$

♠ : in the case of inclusive reactions this attenuation must be compensated

♢ : $\sqrt{\lambda_n}\langle\varphi_n \mid j^{\mu\dagger}(\boldsymbol{q})\sqrt{1-\mathcal{V}'(E)} \mid \tilde{\chi}_{\mathcal{E}}^{(-)}(E)\rangle \Longrightarrow$ gain due to the flux lost towards the channel n by the other final states asymptotically originated by the channels different from n

♣ : usual shell-model calculation: sum, over all the single-particle shell-model states, of the squared absolute value of the transition matrix elements
$\Longrightarrow$ loss of flux that is inconsistent with the inclusive process, where all the inelastic channels must be considered and the total flux must be conserved

♡ : Green's function approach $\Longrightarrow$ the flux is conserved: the loss of flux, produced by the negative imaginary part of the optical potential in χ, is compensated by the gain of flux, produced in the first matrix element by the positive imaginary part of the Hermitian conjugate optical potential in $\tilde{\chi}$

♠ : see A. Meucci, F. Capuzzi, C. Giusti, F.D. Pacati, Phys. Rev. C **67**, 054601 (2003); A. Meucci, C. Giusti, F.D. Pacati, Nucl. Phys. A 739, 277 (2004)

Summary and Conclusions

♡ : Charged- and Neutral-Current neutrino-nucleus scattering

♠ : relativistic models for neutrino-nucleus scattering

♢ : CC scattering ⟶ comparison between RMF and RGF

♣ : results for the MiniBooNE CCQE cross sections ⟶ RMF and RGF

♡ : results for the MiniBooNE NCE cross sections ⟶ RGF

♠ : Thank you very much!